Published OnlineFirst October 27, 2009; DOI: 10.1158/1078-0432.CCR-09-0767
Published Online First on October 27, 2009 as 10.1158/1078-0432.CCR-09-0767

Preclinical Therapy

Reciprocal Regulation of c-Src and STAT3 in Non-Small Cell Lung Cancer

Lauren Averett Byers,[1,2] Banibrata Sen,[2] Babita Saigal,[2] Lixia Diao,[3] Jing Wang,[3] Meera Nanjundan,[7] Tina Cascone,[2] Gordon B. Mills,[4,6] John V. Heymach,[2,5] and Faye M. Johnson[2,6]

Abstract

Purpose: Signal transducer and activator of transcription-3 (STAT3) is downstream of growth factor and cytokine receptors, and regulates key oncogenic pathways in non–small cell lung cancer (NSCLC). Activation of STAT3 by cellular Src (c-Src) promotes tumor progression. We hypothesized that c-Src inhibition could activate STAT3 by inducing a homeostatic feedback loop, contributing to c-Src inhibitor resistance.

Experimental Design: The effects of c-Src inhibition on total and phosphorylated STAT3 were measured in NSCLC cell lines and in murine xenograft models by Western blotting. c-Src and STAT3 activity as indicated by phosphorylation was determined in 46 human tumors and paired normal lung by reverse phase protein array. Modulation of dasatinib (c-Src inhibitor) cytotoxicity by STAT3 knockdown was measured by MTT, cell cycle, and apoptosis assays.

Results: Depletion of c-Src by small interfering RNA or sustained inhibition by dasatinib increased pSTAT3, which could be blocked by inhibition of JAK. Similarly, *in vivo* pSTAT3 levels initially decreased but were strongly induced after sustained dasatinib treatment. In human tumors, phosphorylation of the autoinhibitory site of c-Src (Y527) correlated with STAT3 phosphorylation ($r = 0.64$; $P = 2.5 \times 10^{-6}$). STAT3 knockdown enhanced the cytotoxicity of dasatinib.

Conclusions: c-Src inhibition leads to JAK-dependent STAT3 activation *in vitro* and *in vivo*. STAT3 knockdown enhances the cytotoxicity of dasatinib, suggesting a compensatory pathway that allows NSCLC survival. Data from human tumors showed a reciprocal regulation of c-Src and STAT3 activation, suggesting that this compensatory pathway functions in human NSCLC. These results provide a rationale for combining c-Src and STAT3 inhibition to improve clinical responses. (Clin Cancer Res 2009;15(22):OF1–10)

Lung cancer accounts for 29% of all cancer deaths in the United States, with a 5-year overall survival rate of 15% for all stages (1). Although chemotherapy remains the standard treatment for advanced or metastatic non–small cell lung cancer (NSCLC), response rates do not exceed 35% with frontline therapies and are even lower in the second-line setting (2). Improving our understanding of the signaling pathways that drive tumor behavior is essential for improving clinical outcomes. One potential therapeutic target in NSCLC for which clinical inhibitors have been developed is cellular Src (c-Src; ref. 3). The Src family consists of nonreceptor tyrosine kinases involved in signal transduction in both normal and cancer cells (4). c-Src is the best characterized and most often involved in cancer progression. c-Src overexpression has been shown in multiple tumor types, in which its activation correlates with shorter survival (reviewed in ref. 3). In NSCLC, c-Src is expressed and

Authors' Affiliations: [1]Division of Cancer Medicine and Departments of [2]Thoracic/Head and Neck Medical Oncology, [3]Bioinformatics and Computational Biology, [4]Systems Biology, and [5]Cancer Biology, The University of Texas M.D. Anderson Cancer Center, and [6]The University of Texas Graduate School of Biomedical Sciences at Houston, Houston, Texas; and [7]Department of Cell Biology, Microbiology, and Molecular Biology, University of South Florida, Tampa, Florida

Received 3/29/09; revised 8/6/09; accepted 8/17/09; published OnlineFirst 10/27/09.

Grant support: Physician Scientist Award (to F.M. Johnson); University of Texas Southwestern Medical Center and M.D. Anderson Cancer Center SPORE NIH grant P50 CA070907; Department of Defense grant W81XWH-07-1-0306 01 (PP-1B); Extension of Radiotherapy Research grant P01 CA006294; CCSG functional proteomics core grant P30 CA016672; and Kleberg Center for Molecular Markers. J.V. Heymach is a Damon Runyon-Lilly Clinical Investigator supported in part by the Damon Runyon Cancer Research Foundation (CI 24-04). L.A. Byers is supported in part by the AACR-AstraZeneca-Prevent Cancer Foundation Fellowship for Translational Lung Cancer Research.

The costs of publication of this article were defrayed in part by the payment of page charges. This article must therefore be hereby marked *advertisement* in accordance with 18 U.S.C. Section 1734 solely to indicate this fact.

Requests for reprints: Faye M. Johnson, Department of Thoracic/Head and Neck Medical Oncology, Unit 432, The University of Texas M.D. Anderson Cancer Center, 1515 Holcombe Boulevard, Houston, TX 77030-4009. Phone: 713-792-6363; Fax: 713-792-1220; E-mail: fmjohns@mdanderson.org.

doi:10.1158/1078-0432.CCR-09-0767

Published OnlineFirst October 27, 2009; DOI: 10.1158/1078-0432.CCR-09-0767

Translational Relevance

Cellular Src (c-Src) inhibitors represent an exciting new class of targeted drugs that have shown clinical activity in several disease types. However, despite the fact that c-Src overexpression and activation are associated with worse prognosis in non–small cell lung cancer (NSCLC) and c-Src inhibition leads to a universal and profound inhibition of NSCLC invasion, the cytotoxic effects of c-Src inhibition are variable. Understanding the mechanisms of resistance to these drugs is of critical importance so that they can be used most effectively. In these studies, we show that sustained c-Src-inhibition in NSCLC leads to phosphorylation of its downstream target STAT3 and that knockdown of STAT3 increases cytotoxicity induced by c-Src inhibition. These findings support assessment of combinations of drugs that inhibit STAT3, such as JAK kinase inhibitors, with c-Src inhibitors in NSCLC.

activated in both adenocarcinomas and squamous cell carcinomas (5, 6).

c-Src participates in several normal cellular functions during development and adulthood, including cell cycle progression, immune recognition, adhesion, spreading, migration, apoptosis regulation, and differentiation (reviewed in refs. 3, 7). In cancer cells, constitutive activation of c-Src disregulates many of these processes. Inhibition of c-Src activity using both molecular approaches and pharmacologic inhibitors in multiple cancer cell types has been found to lead to reduced anchorage-independent growth (8), decreased proliferation (9), cell cycle arrest (10), decreased tumor growth *in vivo* (11, 12), apoptosis (9), increased susceptibility to anoikis (13), diminished *in vitro* invasion and migration (14, 15), decreased *in vivo* metastasis (12, 16), and decreased *in vivo* vascularity (17). In NSCLC specifically, c-Src inhibition leads to decreased hypoxia-induced vascular endothelial growth factor expression (18). Inhibition of c-Src with a pharmacologic inhibitor (dasatinib) leads to profound and universal *in vitro* inhibition of migration and invasion of NSCLC cells. However, its effect on viability and proliferation is more variable and occurs at concentrations of dasatinib that are near or above the peak plasma concentrations possible in humans (14).

c-Src has multiple downstream substrates that mediate its biological functions in cancer cells. The interaction between c-Src and its substrate focal adhesion kinase (FAK) is essential for normal cell migration and invasion (19). c-Src also regulates downstream proliferation induced by growth factor receptors. Following activation by growth factor receptors, c-Src promotes survival via phosphorylation of the p85 subunit of phosphatidylinositide 3 kinase (PI3K) and thus the AKT pathway, signal transducer and activator of transcription-3 (STAT3), STAT5, and Shc, and thus the Ras/mitogen-activated protein kinase pathway (13, 20, 21). The STAT family of transcription factors, especially STAT3, regulates oncogenic signaling in many different tumor types (22). Indeed STAT3 is required for viral Src-mediated transformation (23). STAT3 can be activated by growth factor receptors or cytokine receptors, usually via non-receptor tyrosine kinases such as c-Src or janus-activated kinase (JAK) proteins. STAT3 activation leads to the increased expression of downstream targets (e.g., Bcl-XL, cyclin D1, survivin) and increased cell survival, proliferation, and tumor growth *in vivo* (24). Inhibition of STAT3 results in increased apoptosis, decreased proliferation, and decreased tumor size (25, 26). STAT3 activation can also contribute to angiogenesis (27). Hypoxia-induced vascular endothelial growth factor expression is dependent on c-Src activation; this activation of c-Src leads to the downstream activation of STAT3, which binds to the vascular endothelial growth factor promoter with hypoxia-inducible factor-1α (HIF-1α).

Although targeting growth factors and signal transduction pathways is a successful strategy in several tumor types, feedback and parallel signaling pathways can limit the efficacy of this approach. Despite c-Src expression in epithelial tumors, including NSCLC, and robust inhibition of c-Src with clinically relevant agents (e.g., dasatinib), the effect of c-Src inhibition on cell survival and proliferation has been modest (14). Defining mechanisms that limit the cytotoxic effects of c-Src inhibitors may result in the development of combinations of therapeutic agents for NSCLC that inhibit metastasis and enhance cytotoxicity. Because c-Src mediates its effects on cancer cell survival and proliferation via diverse substrates, including STATs, in this study we tested our hypothesis that STAT3 may not be inhibited sufficiently by c-Src inhibition in NSCLC to result in clinical effects. We determined that STAT3 was not durably inhibited in NSCLC cell lines and xenografts following c-Src inhibition, making it a candidate pathway for resistance to chemotherapy. Consistent with this result, we found that depletion of STAT3 enhanced the cytotoxicity of c-Src inhibition. In addition, we observed an inverse correlation between c-Src and STAT3 activation levels in untreated primary lung tumors by reverse-phase protein array. The results of these studies support a model in which c-Src and STAT3 are reciprocally regulated in NSCLC tumors, allowing for cancer cell survival following c-Src inhibition.

Materials and Methods

Pharmacologic inhibitors. Dasatinib for *in vitro* studies was provided by Bristol-Myers Squibb and was prepared as a 10 mmol/L stock solution in DMSO. Dasatinib for animal studies was purchased from The University of Texas M. D. Anderson Cancer Center pharmacy. Pyridone 6 was purchased from Calbiochem.

Cell line selection and culture. Human NSCLC cell lines A549 and H226 were obtained from the American Type Culture Collection. H1299, H2009, and H1792 were gifts from Dr. John Minna (Hamon Center for Therapeutic Oncology Research, University of Texas Southwestern Medical Center, Dallas, Texas). Cell lines with wild-type epidermal growth factor receptors (EGFR) were selected for these studies because EGFR mutations can profoundly affect the response of NSCLC to c-Src inhibition. Three KRAS mutant cell lines were included (A549, H2009, and H1792) because this mutation is common in patients with NSCLC. Cells were grown in monolayer cultures in RPMI 1640 medium containing 10% fetal bovine serum (A549, H226, H1299, and H1792) or RPMI 1640 medium supplemented with hydrocortisone, insulin, transferrin, estadiol, and selenium (HITES) containing 5% fetal bovine serum (H2009) at 37°C in a humidified atmosphere of 95% air and 5% CO_2.

Western blot analysis. Western blot analysis was done to measure protein expression and phosphorylation at 30 min and 7 h after inhibition or specific knockdown of c-Src, STAT3, and/or JAK. Protein levels in treated cells were compared with those in untreated cells at these

Published OnlineFirst October 27, 2009; DOI: 10.1158/1078-0432.CCR-09-0767

same times to control for the effect of confluence or vehicle effects on STAT3 activation. Antibodies used in the Western blot analysis included c-Src and pSTAT3 S727 (Santa Cruz Biotechnology); pSrc Y419, pSTAT3 Y705, STAT3, pFAK Y861, Lyn, Yes, Bcl-XL, survivin, and STAT5 (Cell Signaling Technology); and β-actin (Sigma Chemical Company).

For the Western blot analysis, cells were rinsed and lysed as previously described (28). Equal protein aliquots from cleared lysates were resolved by SDS-PAGE, transferred to nitrocellulose membranes, immunoblotted with primary antibody, and detected with horseradish peroxidase–conjugated secondary antibody (Bio-Rad Laboratories) and enhanced chemiluminescence reagent (Amersham Biosciences).

Transfection with small interfering RNA. To knock down STAT3, the NSCLC cells were harvested, washed, and suspended at a density of 1 million cells/100 μL of Nucleofector-V solution (Amaxa Corp.). Small interfering RNA (siRNA; 200 pmol/100 μL) was added to the cell suspension and electroporated using the U-31 Nucleofector program (Amaxa). Immediately after electroporation, 500 μL of prewarmed RPMI medium were added to the cuvette, and the cells were transferred to 6-well plates. The medium was changed after 16 h. STAT3 and c-Src siRNA were predesigned by siGenome Smartpool (Dharmacon, Inc., a part of Thermo Fisher Scientific) and obtained from Ambion. Controls included cells that were mock-transfected (i.e., without siRNA) and those transfected with a nontargeting (scrambled) siRNA.

MTT, cell cycle, and apoptosis assays. The MTT assay was used to assess cytotoxicity as previously described (28). For each cell line, eight wells were treated with 0, 1, 2, 4, or 8 μmol/L dasatinib and the IC_{50}. Cell cycle analysis was done as described previously (29). Briefly, cells were fixed and stained with propidium iodide. DNA content was analyzed by fluorescence-activated cell sorting analysis (Becton Dickinson) using ModFit software (Verity Software House). Apoptosis was measured using terminal deoxynucleotidyl transferase biotin-dUTP nick-end labeling staining using the manufacturer's protocol (APO-BRDU kit, Phoenix Flow Systems) as described previously (30). Briefly, fixed cells were incubated with terminal deoxynucleotidyl transferase and Br-dUTP and subsequently incubated with a fluorescein-labeled anti–Br-dUTP antibody and analyzed by fluorescence-activated cell sorting analysis.

Xenograft nude mouse models. All animal procedures were done in accordance with the policies of M.D. Anderson's Institutional Animal Care and Use Committee. Ten female Swiss *nu/nu* strain, 6-week-old mice were used for each xenograft model. Each athymic nude mouse was injected s.c. with 4 million A549 or H226. When visible tumors had developed, dasatinib was administered by oral gavage at a dose of 20 mg/kg/d for 5 d. The mice were euthanized 2 h after the last dose of dasatinib, tumors were dissected, and the mice were examined for distant metastases. The tumors were homogenized and subjected to Western blotting as previously described (30).

Human NSCLC Tumors. Forty-six paired normal lung and NSCLC tumor samples were obtained from surgical specimens in the M. D. Anderson Cancer Center Thoracic Tissue Bank (Table 1). Of the tumors, 22 were squamous cell carcinomas and 24 were adenocarcinomas. The median age of the patients from whom the tumors had been excised was 67 y (range, 48-81 y); 22 (48%) were women, and 44 (96%) were former or current smokers. Six (13%) patients had stage IA cancer, 14 (30%) stage IB, 2 (4%) stage IIA, 13 (28%) stage IIB, 3 (7%) stage IIIA, 6 (13%) stage IIIB, and 2 (4%) stage IV.

Reverse-phase protein array. Protein lysate was prepared from pellets from tumor tissues as previously described (31). Briefly, lysis buffer [1% Triton X-100, 50 mmol/L HEPES (pH 7.4), 150 mmol/L NaCl, 1.5 mmol/L $MgCl_2$, 1 mmol/L EGTA, 100 mmol/L NaF, 10 mmol/L NaPPi, 10% glycerol, 1 mmol/L phenylmethylsulfonyl fluoride, 1 mmol/L Na_3VO_4, and 10 μg/mL aprotinin] was added to the samples, followed by microcentrifugation at 14,000 rpm for 10 min. Clear supernatants were collected, followed by protein quantitation using the BCA reaction kit (Pierce Biotechnology, Inc.). The cell lysate was mixed with SDS sample buffer without bromophenol blue [three parts cell lysate plus one part 4× SDS sample buffer, which contained 35% glycerol, 8% SDS, 0.25 mol/L Tris-HCl (pH 6.8)]. Before using the cell lysate, 10% β-mercaptoethanol was added. The samples were boiled for 5 min. Then, the samples (each in duplicate) were serially diluted (1:2-1:16) with SDS sample buffer. To each of the diluted samples an equal amount of 80% glycerol/2× PBS solution (8 mL of glycerol mixed with 2 mL of 10× PBS without Ca^{2+} and Mg^{2+}) was added, after which the diluted samples were transferred to 384-well plates. Reverse-phase protein arrays (RPPA) were produced and analyzed as described (52), with slight modifications. Protein arrays were printed on nitrocellulose-coated glass FAST Slides (Schleicher & Schuell BioScience Inc.) by a GeneTAC G3 arrayer (Genomic Solutions) with 48 200-μm-diameter pins arranged in a 4 × 12 format. Forty-eight grids were printed at each slide with each grid containing 24 dots. Protein dots were printed in duplicate with five concentrations. Arrays were produced in batches of 15, and occasional low-quality arrays (e.g., with many spot dropouts) were discarded.

Antibody staining of each array was done using an automated BioGenex autostainer. Briefly, each array was incubated with a specific primary antibody: pSrc Y527, pSTAT3 Y705, pSrc Y416 (which binds the pSrc Y419 activation site in humans), pFAK Y576, p-p130Cas Y249, and pPaxillin Y118; Cell Signaling); c-Src and STAT3 (Upstate). The signal was detected using the catalyzed signal amplification (CSA) system according to the manufacturer's recommended procedure (DakoCytomation California, Inc.). In brief, the RPPA slides were blocked for endogenous peroxidase, avidin, and biotin protein activity with I-block (Applied Biosystems) at room temperature for 15 min. After the blocking procedure, the slides were incubated with primary antibody and secondary antibody and diluted in DAKO antibody diluent with a background-reducing compound at room temperature for 20 min each. The slides were then incubated with streptavidin-biotin complex and biotinyl-tyramide (for amplification) for 15 min each, streptavidin-peroxidase for 15 min, and 3,3-diaminobenzidine tetrahydrochloride chromogen for 5 min. Between steps, each slide was washed with TBS containing 0.1% Tween-20 (TBST). Spot images were quantified using imaging analysis with an HP Scanjet 8200 scanner (Hewlett Packard) with a 256-shade gray scale at 600 dots per inch.

RPPA data processing and statistical analysis. RPPA data were quantified using a SuperCurve method which detects changes in protein level by Microvigene software (VigeneTech) and an R package developed in-house (32). Briefly, the SuperCurve method generates a common logistic curve by pooling data from all samples on the slide. Individual dilution series numbers for each sample are then mapped onto the SuperCurve for quantification. After quantification, data were logarithm-transformed (base 2) for further processing and analyses. Then median-control normalization was applied on the dataset. The statistical analyses were done using R (version 2.7.0). All samples were done in duplicate, and average values were used for analysis. Two sample *t*-tests were used to compare protein levels between normal and tumor tissue; Pearson correlations were used to analyze the association between protein levels in the samples. In all analyses, $P \leq 0.05$ was considered significant.

Results

c-Src inhibition fails to durably inhibit STAT3 in NSCLC cell lines. Western blot analysis of five NSCLC cell lines showed that c-Src phosphorylation was rapidly (30 minutes) and durably (7 hours) inhibited at a site essential for c-Src activation (pSrc Y419 in human c-Src; Fig. 1A). Total c-Src levels were not changed by dasatinib treatment. In contrast to pSrc Y419, in which inhibition was prolonged, STAT3 activation (as shown by pSTAT3 Y705 levels) was transiently inhibited at 30 minutes in A549 and H226 (0.60 and 0.57 times the control value, respectively), followed by reactivation by 7 hours (1.25 and 1.18 times control). In H2009, H1299, and H1792 activation was

Published OnlineFirst October 27, 2009; DOI: 10.1158/1078-0432.CCR-09-0767

Table 1. Clinicopathologic characteristics of patients included in RPPA analysis of NSCLC tumors

Specimen number	Histology	Age at surgery, y	Gender	Race	Smoking status	T stage	N stage	M stage	Overall stage
700	SQ	79	M	Caucasian	Former	T_2	N_1	M_0	IIB
708	SQ	61	F	African American	Never	T_2	N_1	M_0	IIB
719	SQ	76	M	Caucasian	Former	T_2	N_0	M_0	IB
720	SQ	67	F	Caucasian	Current	T_1	N_1	M_0	IIA
739	AD	76	F	Caucasian	Former	T_2	N_2	M_1	IV
746	AD	67	F	Caucasian	Former	T_4	N_0	M_0	IIIB
759	AD	60	M	Caucasian	Current	T_2	N_2	M_0	IIIB
763	AD	60	F	Caucasian	Current	T_2	N_2	M_0	IIIA
764	AD	67	F	Caucasian	Current	T_2	N_0	M_0	IB
767	AD	53	F	African American	Current	T_1	N_2	M_0	IIIA
771	SQ	67	M	Caucasian	Former	T_2	N_1	M_0	IIB
773	AD	77	F	Caucasian	Former	T_4	N_2	M_1	IV
774	SQ	67	M	African American	Former	T_4	N_2	M_0	IIIB
781	SQ	80	F	Caucasian	Former	T_1	N_0	M_0	IA
782	AD	67	M	Caucasian	Former	T_4	N_0	M_0	IIIB
786	SQ	81	M	Caucasian	Former	T_2	N_1	M_0	IIB
795	AD	64	M	Caucasian	Never	T_1	N_0	M_0	IA
799	SQ	61	F	Caucasian	Current	T_2	N_0	M_0	IB
801	AD	63	F	Caucasian	Current	T_2	N_1	M_0	IIB
803	AD	65	F	African American	Current	T_2	N_1	M_0	IIB
804	SQ	77	M	Caucasian	Former	T_2	N_0	M_0	IB
811	SQ	62	M	Caucasian	Current	T_2	N_1	M_0	IIB
813	SQ	70	M	Caucasian	Current	T_4	N_0	M_0	IIIB
816	AD	73	M	Caucasian	Former	T_2	N_0	M_0	IB
833	AD	72	M	Caucasian	Current	T_1	N_0	M_0	IA
844	SQ	67	M	Caucasian	Former	T_2	N_1	M_0	IB
847	AD	60	F	Caucasian	Current	T_2	N_0	M_0	IB
848	AD	48	F	Caucasian	Current	T_2	N_0	M_0	IB
849	AD	57	M	Caucasian	Current	T_1	N_1	M_0	IIA
852	SQ	67	M	Caucasian	Current	T_2	N_0	M_0	IB
857	SQ	71	M	Caucasian	Current	T_2	N_0	M_0	IB
870	SQ	53	M	Caucasian	Current	T_2	N_1	M_0	IIB
877	AD	68	M	Caucasian	Former	T_2	N_1	M_0	IIB
879	SQ	67	M	Caucasian	Current	T_2	N_1	M_0	IIB
883	AD	58	F	Caucasian	Former	T_2	N_1	M_0	IIB
884	AD	70	F	Caucasian	Former	T_1	N_0	M_0	IA
890	AD	68	M	Caucasian	Former	T_2	N_0	M_0	IB
896	AD	49	F	Caucasian	Current	T_1	N_0	M_0	IA
899	AD	65	F	Caucasian	Current	T_1	N_0	M_0	IA
905	SQ	80	M	Caucasian	Former	T_2	N_1	M_0	IIB
910	AD	74	F	Caucasian	Former	T_2	N_0	M_0	IB
911	SQ	65	F	Caucasian	Former	T_2	N_0	M_0	IB
913	SQ	61	M	Caucasian	Former	T_2	N_2	M_0	IIIA
920	AD	54	F	Caucasian	Current	T_2	N_0	M_0	IB
930	SQ	66	M	Caucasian	Former	T_2	N_1	M_0	IIB
931	SQ	71	F	Caucasian	Current	T_4	N_0	M_0	IIIB

Abbrevations: AD, adenocarcinoma; SQ, squamous cell carcinoma.

seen beginning at 30 minutes (range, 1.20-1.78 times control) and persisted at 7 hours (1.19-1.63 times control; Fig. 1B).

***c-Src inhibition leads to initial STAT3 inhibition then reactivation* in vivo.** After 1, 5, or 7 hours and after 5 days of dasatinib treatment, tumors from mouse xenografts of NSCLC cells were grossly dissected and examined by immunohistochemistry. Tumors were confirmed to consist primarily of NSCLC cells (>90%) with no distant metastases (data not shown). Protein expression and phosphorylation were then measured by Western blot analysis and compared with control (vehicle-treated mice sacrificed at 7 hours or 5 days; Fig. 2). As expected, dasatinib treatment resulted in pSrc Y419 inhibition at all times. In A549 xenografts, pFAK inhibition was seen beginning at 5 hours. In contrast, but consistent with the *in vitro* data, pSTAT3 Y705 was inhibited at early times (0.58-fold at 5 hours after treatment) but was strongly induced by 7 hours (3.1-fold). pSTAT3 Y705 levels returned to baseline after 5 days of continuous daily treatment. Unlike the *in vitro* studies, the *in vivo* studies showed that total STAT3 levels were also elevated at 7 hours after treatment but were not significantly different from

Published OnlineFirst October 27, 2009; DOI: 10.1158/1078-0432.CCR-09-0767

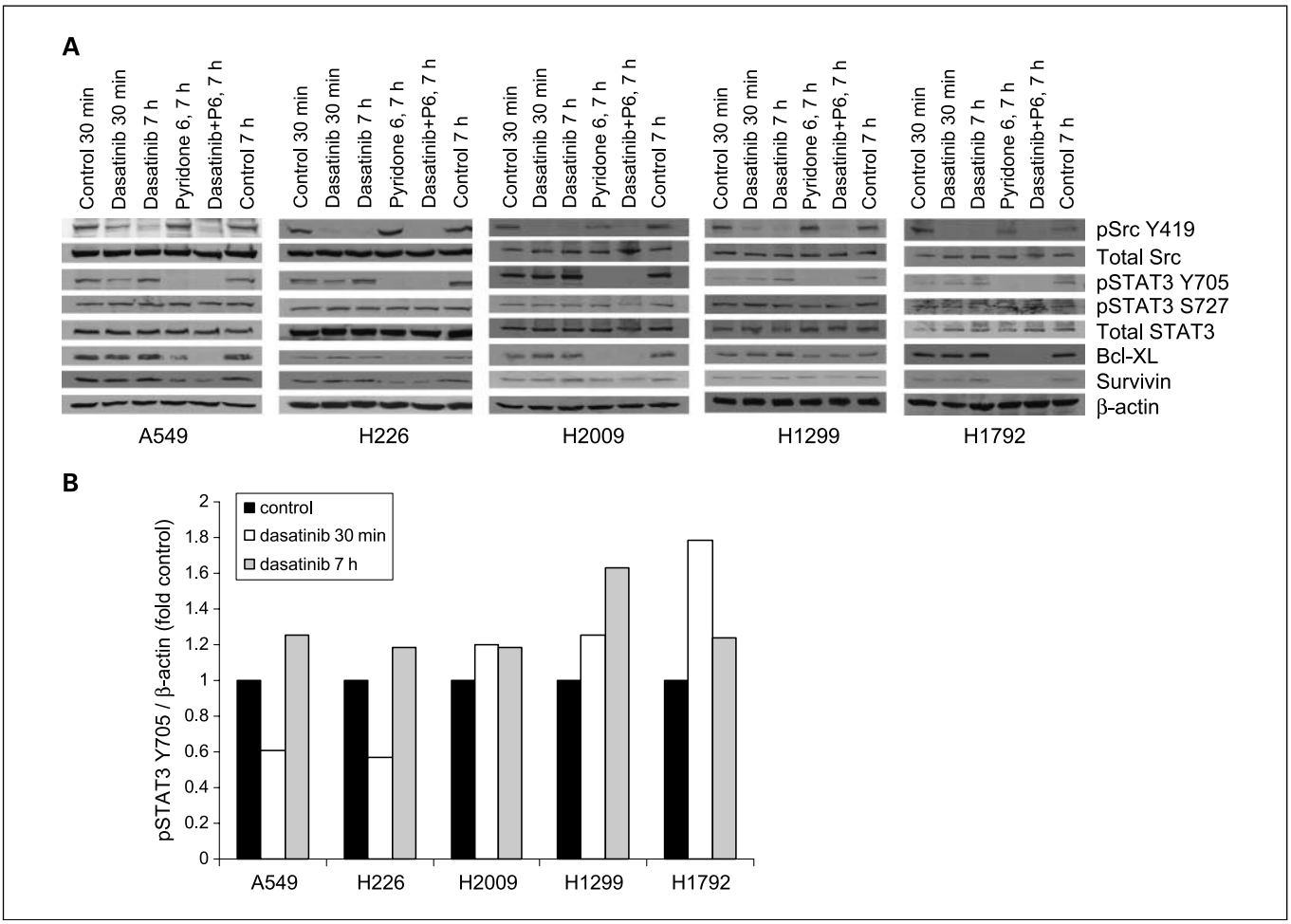

Fig. 1. c-Src inhibition fails to durably inhibit pSTAT3 Y705 *in vitro*. Activation of pSTAT3 Y705 following dasatinib treatment is inhibited by the addition of the JAK inhibitor pyridone 6 (P6). *A,* NSCLC cells were incubated with 100 nmol/L dasatinib, 2.5 μmol/L pyridone 6, both drugs, or vehicle alone (control) for the indicated times, lysed, and analyzed by Western blotting with the indicated antibodies. *B,* changes in pSTAT3 Y705 were quantified using densitometry. pSTAT3 Y705 levels were normalized to total β-actin and the degree of change was measured between dasatinib-treated cells and control cells corresponding to the same time point (30 min or 7 h).

control levels. In H226 xenografts, pSTAT3 Y705 was inhibited between 5 and 7 hours (0.32- and 0.44-fold at 5 and 7 hours, respectively), but rose above baseline by 5 days (1.7-fold).

c-Src depletion leads to STAT3 activation. To determine whether STAT3 reactivation was downstream of c-Src and not caused by an off-target effect of dasatinib, we examined the effect of c-Src depletion by siRNA at 72 and 96 hours in the NSCLC cell lines A549 and H226. Cell lines were transfected with either scrambled siRNA or c-Src–specific siRNA. In A549 cells, c-Src knockdown decreased total and activated c-Src levels but increased pSTAT3 Y705 by 6.7- and 7.2-fold at 72 and 96 hours, respectively (Fig. 3). In H226 cells, total and activated c-Src levels were suppressed at both time points; pSTAT Y705 was strongly induced by 72 hours (3.5-fold) and returned near baseline by 96 hours (1.5-fold; Fig. 3). Other Src family members, such as Yes and Lyn, were not affected by c-Src knockdown in either cell line.

STAT3 reactivation is JAK-dependent. To determine whether STAT3 reactivation was mediated by JAK proteins, we tested the effect of JAK inhibition on STAT3 activation. NSCLC cell lines were treated with the JAK inhibitor pyridone 6 alone and in combination with dasatinib (Fig. 1A). JAK inhibition alone had no effect on pSrc Y419 but led to complete inhibition of pSTAT3 Y705 and its downstream targets survivin and Bcl-XL at 7 hours. When combined with dasatinib, JAK inhibition by pyridone 6 prevented STAT3 phosphorylation.

c-Src and STAT3 are reciprocally regulated in NSCLC patient tumors. To evaluate the relationship between c-Src and STAT3 in clinical samples, we used reverse-phase protein array, due to its sensitivity and the small amount of protein required, to quantify the levels of total and phosphorylated Src and STAT3 as well as downstream targets of Src in paired samples of NSCLC tumors and normal lung tissue. Paired *t*-test of tumor and normal tissue from the same patients showed significantly higher c-Src activity in tumors as illustrated by decreased levels of autophosphorylated and inactive c-Src (pSrc Y527; $P = 1.09 \times 10^{-9}$) in tumor tissue as compared with normal lung (Fig. 4A). In contrast, activated STAT3 (pSTAT3 Y705) levels were significantly lower in tumor tissue ($P = 0.006$; Fig. 4A).

Among the tumor specimens, there was a statistically significant correlation between levels of pSrc Y527 and pSTAT3 Y705, with a Pearson correlation coefficient of 0.32 ($P = 0.03$; Fig. 4B). This correlation was also seen when the ratio of pSrc Y527 to total c-Src in tumors was compared with the ratio of

Published OnlineFirst October 27, 2009; DOI: 10.1158/1078-0432.CCR-09-0767

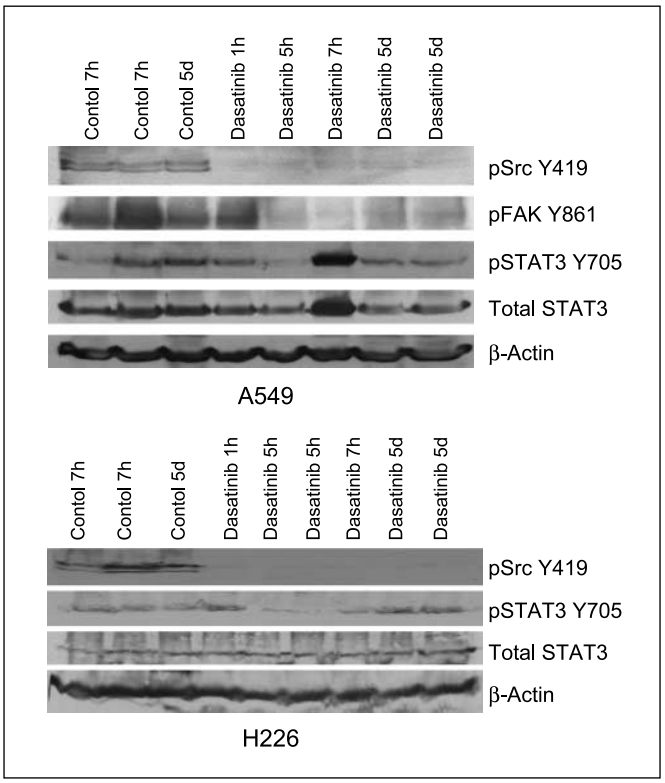

Fig. 2. c-Src inhibition results in STAT3 reactivation *in vivo*. A549 and H226 xenografts were treated daily with dasatinib at 20 mg/kg/d or with vehicle. Tumors were lysed at the times shown and analyzed by Western blotting with the indicated antibodies.

pSTAT3 Y705 to total STAT3 ($r = 0.56$; $P = 5.25 \times 10^{-5}$; Fig. 4B). In addition, the decrease in pSrc Y527 from normal to tumor correlated directly with the decease in pSTAT3 Y705 from normal to tumor tissue ($r = 0.33$; $P = 0.03$).

Downstream targets of Src (FAK, p130Cas, and paxillin) were also evaluated by RPPA. As expected, activation of these targets (as measured by phosphorylation) was inversely correlated with pSTAT3 Y705 and pSrc Y527. Specifically, correlation coefficients between pSTAT3 Y705 and phosphorylated FAK, p130Cas, and paxillin were $r = -0.50$ ($P = 0.0005$), -0.30 ($P = 0.04$), and -0.42 ($P = 0.004$), respectively (Fig. 4C).

Despite testing several antibodies for RPPA, there is not yet a validated antibody for this assay for the activated form of c-Src (human pSrc Y419). However, using the best performing antibody available, we observed a 1.6-fold higher level of pSrc Y419 in tumors compared with normal tissue ($P = 0.06$). The ratio of pSrc Y419 to total Src was also correlated with the ratio of pSTAT3 Y705 to total STAT3, although this was not statistically significant ($P = 0.67$).

Inhibition of STAT3 with siRNA enhances the cytotoxicity of dasatinib. Because of its role in mediating survival and proliferation, STAT3 induction following c-Src inhibition may represent a mechanism of drug resistance. To examine the biological effects of STAT3 reactivation in NSCLC cells, we evaluated the effect of STAT3 knockdown on cytotoxicity when combined with dasatinib. A549 and H226 cells were transfected with STAT3 siRNA, scrambled (nontargeting) siRNA, or mock-transfected. A549 and H226 cells transfected with STAT3 siRNA showed an 87% and 79% decrease in STAT3 protein levels (respectively) at 48 hours after transfection with STAT3 siRNA as compared with scrambled siRNA (Fig. 5A and B). To determine the biological effect of c-Src inhibition combined with specific depletion of STAT3, cells were treated with dasatinib 48 hours after transfection. A MTT assay was then used to estimate the number of living cells remaining after 72 hours of treatment. Cells with depleted STAT3 were significantly more sensitive to dasatinib than those transfected with scrambled siRNA. In A549 cells, the IC_{50} values were 0.7 and 4 μmol/L in control and STAT3 siRNA–transfected cells, respectively, for A549 (Fig. 5C), and 5 and 38 μmol/L for H226 (Fig. 5D). Unlike dasatinib alone, the combination of STAT3 knockdown with dasatinib strongly induced apoptosis in both cell lines (Fig. 5E). Dasatinib alone induced cell cycle arrest in H226 cells, but this was not significantly affected by the addition of STAT3 depletion.

Discussion

In this study, we found that c-Src and STAT3 activation, as shown by phosphorylation status, were reciprocally regulated in NSCLC cell lines, xenografts, and human tumors. Despite an initial inhibition of STAT3 phosphorylation in the A549 and H226 models, prolonged c-Src inhibition resulted in an increase in STAT3 phosphorylation in all NSCLC cell lines tested both *in vitro* and *in vivo*. STAT3 reactivation was JAK-dependent, as illustrated by the observation that reactivation was inhibited by the addition of a JAK inhibitor, pyridone 6. Finally, we showed that inhibition of STAT3 reactivation (by STAT3 siRNA) enhanced the cytotoxicity of dasatinib, showing that this pathway has biological significance. Taken together, these results suggest that STAT3 reactivation may be an important mechanism of resistance to c-Src inhibitors in NSCLC and may be a clinically relevant target for combination therapy.

Previous studies have shown that c-Src is overexpressed in NSCLC and that increased c-Src activity is associated with worse clinical outcome. Clinical investigators are enthusiastic about c-Src inhibitors because specific and potent kinase inhibitors are well tolerated in humans (33). Two such approved anticancer drugs, imatinib and erlotinib, use ATP-competitive kinase

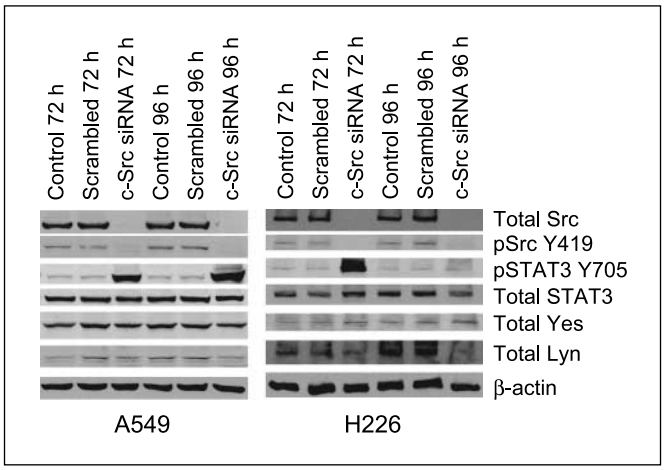

Fig. 3. c-Src depletion results in STAT3 reactivation *in vitro*. A549 and H226 cells were transfected with c-Src–specific siRNA or nontargeting (scrambled) siRNA. Control cells were mock-transfected. Cells were lysed at 72 h or 96 h and analyzed by Western blotting.

Published OnlineFirst October 27, 2009; DOI: 10.1158/1078-0432.CCR-09-0767

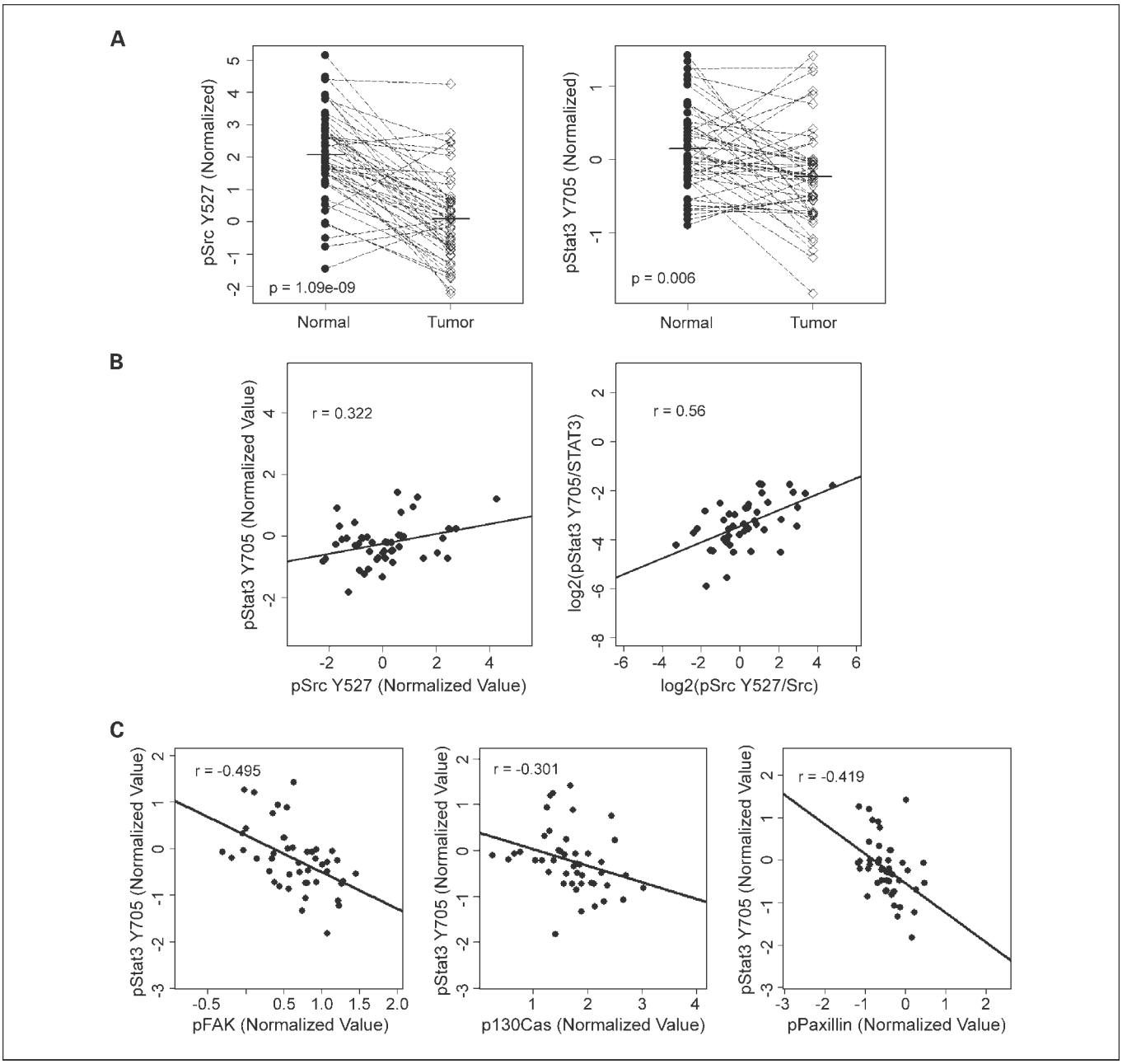

Fig. 4. Phosphorylated c-Src, STAT3, and downstream Src targets were measured in paired normal lung and NSCLC tumor tissues from patients who had previously undergone resection. *A,* tumors had higher mean c-Src activity, as indicated by decreased levels of inactive c-Src (pSrc Y527). Conversely, mean activated STAT3 (pSTAT3 Y705) was lower in tumor tissue than in normal lung. *B,* levels of inactive c-Src (pSrc Y527) correlated directly with activated STAT3 (pSTAT3 Y705) when analyzed as total levels of phosphorylated protein or ratio of phosphorylated protein to total protein. *C,* levels of phosphorylated FAK, p130Cas, and paxillin were inversely correlated with pSTAT3 Y705.

inhibition to inhibit Bcr-Abl (34) and EGFR (35), respectively, proving that kinase inhibition of signal transduction molecules can lead to profound tumor responses. However, thus far c-Src inhibitors have shown limited activity in NSCLC patients. Understanding the mechanisms of resistance to c-Src inhibition in NSCLC will be extremely important for understanding how these drugs can be used more effectively in this disease.

In NSCLC, resistance to tyrosine kinase inhibitors, such as those targeting EGFR, is often due to either activation of the signaling pathway downstream to the drug target (e.g., k-Ras mutations) or signaling through alternate pathways (e.g., c-Met; refs. 36, 37). Therefore, because STAT3 activity is an important downstream target of c-Src and necessary for c-Src signal transduction, characterization of its relationship to c-Src activity and response to c-Src inhibition was of particular interest. Interesting, these studies did show reactivation of STAT3 in the setting of c-Src inhibition. In cell lines from head and neck squamous cell cancers (30), squamous cell carcinoma of the skin,[8] and mesothelioma (38), sustained c-Src inhibition also resulted in STAT3 reactivation. This suggests that reciprocal c-Src-STAT3 regulation

[8] Unpublished data.

Published OnlineFirst October 27, 2009; DOI: 10.1158/1078-0432.CCR-09-0767

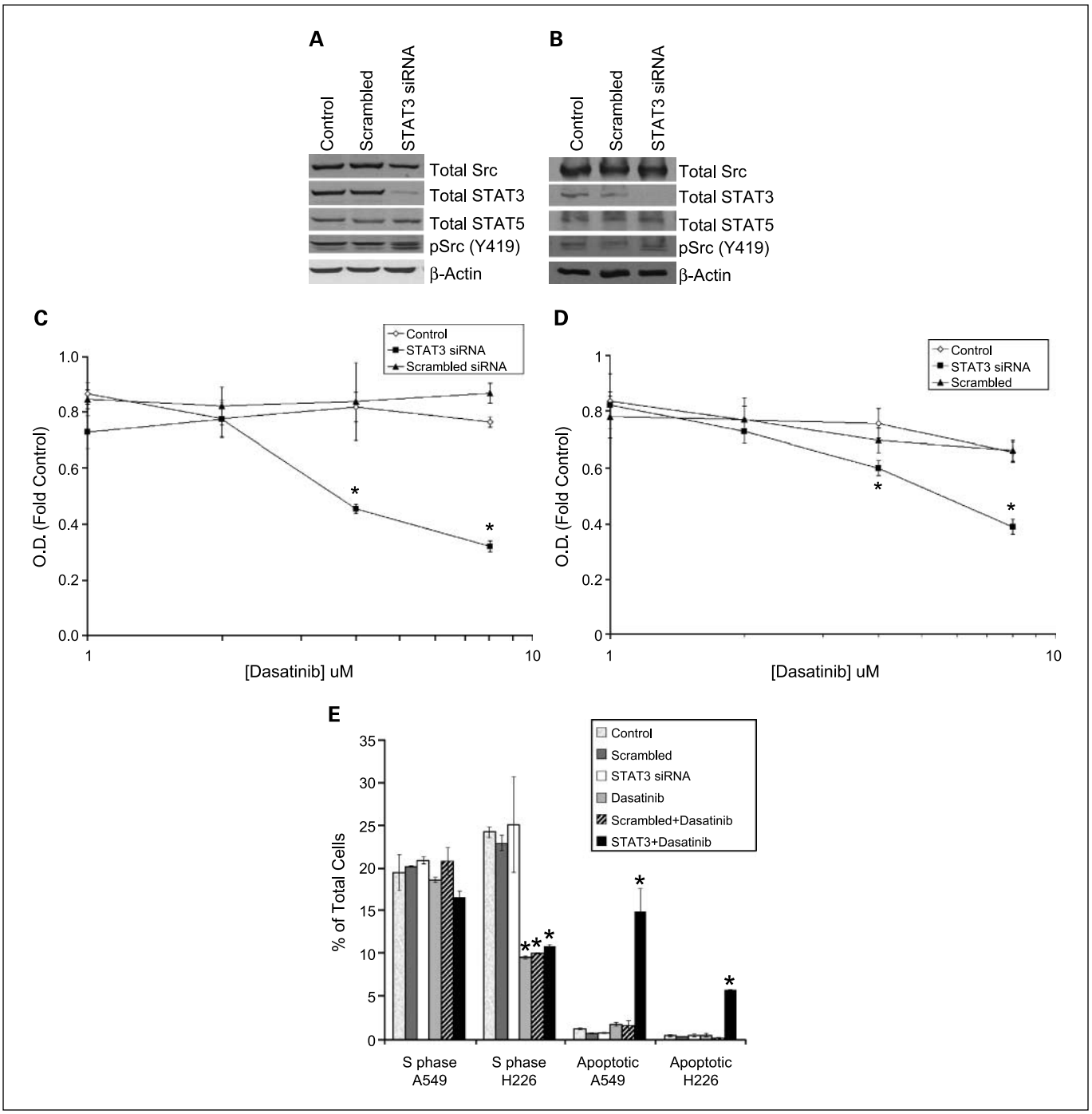

Fig. 5. Depletion of STAT3 enhances cytotoxicity of dasatinib. A549 (*A*) and H226 (*B*) cells were transfected with STAT3-specific siRNA, scrambled siRNA, or mock-transfected. Forty-eight hours after transfection, cells were treated with various concentrations of dasatinib. The number of viable A549 (*C*) and H226 (*D*) cells after 72 h was evaluated by MTT assay. The percentage of cells in S phase and in apoptosis were then measured under the conditions shown. The control sample was compared with each treatment group and significant differences ($P < 0.05$) are marked with an asterisk (*E*).

exists in multiple tumor types. However, this is the first study to show reciprocal regulation of c-Src and STAT3 in patient tumors.

Three negative feedback loops regulate STAT function after cytokine signaling: SH-2–containing phosphatases, which inactivate JAK by dephosphorylation; protein inhibitors of activated STAT, which are negative regulators of STAT-induced transcription (i.e., downstream of STATs); and suppressors of cytokine signaling, which inhibit JAK activity, facilitate proteosomal degradation of JAK, and compete with STATs for binding to cytokine receptors (39). Although there are no known positive feedback loops leading to STAT3 activation after its inhibition, loss of a negative feedback loop could play the same role. For example, v-Abl leads to JAK/STAT activation via its disruption of suppressor of cytokine signaling 1 function (SOCS-1) (40).

The concentration (100 nmol/L) of dasatinib was chosen for these studies because it has been shown to completely inhibit c-Src and is relatively specific (41). For example, in intact cells, we observed ~90% reduction in phosphorylated

Published OnlineFirst October 27, 2009; DOI: 10.1158/1078-0432.CCR-09-0767

c-Src with >40 nmol/L dasatinib.[9] In patients treated with dasatinib, plasma levels of approximately 400 nmol/L were reached with sustained levels of 40 to 100 nmol/L (42, 43), supporting the clinical relevance of our selected drug concentration. However, at these concentrations dasatinib also inhibits Abl, PDGFR, Btk, and EphA2 (44, 45). To determine that STAT3 reactivation is downstream of c-Src specifically and not due to an off-target effect of dasatinib, we showed that when c-Src was depleted by siRNA, the levels of pSrc decreased significantly, but pSTAT3 levels increased.

Although we showed an inverse correlation between c-Src and STAT3 activity in human tumors, human NSCLC samples were not available from the post-dasatinib setting to confirm a reactivation of STAT3 in patients following c-Src inhibition. Nevertheless, we believe that our *in vitro* and murine models sufficiently support a rationale for combining c-Src and STAT inhibition in the clinical setting. Three ATP-competitive c-Src inhibitors are being studied in clinical trials: dasatinib, AZD0530 (AstraZeneca), and SKI-606 (Wyeth). A non–ATP-competitive c-Src inhibitor is also in clinical trial (Kinex pharmaceuticals). Preclinical studies of c-Src inhibitor AZD0530 also showed a reactivation of STAT3 in A549 cells 24 hours after treatment with this drug, further supporting that this may be an important mechanism of resistance across this class of drugs (46). Many JAK inhibitors are being studied in the laboratory and several are in early clinical trial (47–50). Our long-term goal is to use the results of these studies to design clinical trials of these or other more specific c-Src and JAK inhibitors, as available, to improve the survival of patients with NSCLC.

[9] Unpublished data.

Disclosure of Potential Conflicts of Interest

No potential conflicts of interest were disclosed.

Acknowledgments

We thank Doris R. Siwak for her contribution to the RPPA experiments.

References

1. American Cancer Society. Cancer facts & figures 2008. Atlanta: American Cancer Society; 2008.
2. Minna J, Schiller J. In: Kasper DFA, Longo DL, editors. Harrison's principles of internal medicine. 17 ed. New York: McGraw-Hill Medical; 2008.
3. Johnson FM, Gallick GE. SRC family nonreceptor tyrosine kinases as molecular targets for cancer therapy. Anticancer Agents Med Chem 2007;7:651–9.
4. Thomas SM, Brugge JS. Cellular functions regulated by Src family kinases. Annu Rev Cell Dev Biol 1997;13:513–609.
5. Zhang J, Kalyankrishna S, Wislez M, et al. SRC-family kinases are activated in non-small cell lung cancer and promote the survival of epidermal growth factor receptor-dependent cell lines. Am J Pathol 2007;170:366–76.
6. Masaki T, Igarashi K, Tokuda M, et al. pp60(c-src) activation in lung adenocarcinoma. Eur J Cancer 2003;39:1447–55.
7. Yeatman TJ. A renaissance for SRC. Nat Rev Cancer 2004;4:470–80.
8. Laird AD, Li G, Moss KG, et al. Src family kinase activity is required for signal tranducer and activator of transcription 3 and focal adhesion kinase phosphorylation and vascular endothelial growth factor signaling *in vivo* and for anchorage-dependent and -independent growth of human tumor cells. Mol Cancer Ther 2003;2:461–9.
9. Niu G, Bowman T, Huang M, et al. Roles of activated Src and Stat3 signaling in melanoma tumor cell growth. Oncogene 2002;21:7001–10.
10. Moasser MM, Srethapakdi M, Sachar KS, Kraker AJ, Rosen N. Inhibition of Src kinases by a selective tyrosine kinase inhibitor causes mitotic arrest. Cancer Res 1999;59:6145–52.
11. Fleming RY, Ellis LM, Parikh NU, Liu W, Staley CA, Gallick GE. Regulation of vascular endothelial growth factor expression in human colon carcinoma cells by activity of src kinase. Surgery 1997;122:501–7.
12. Trevino JG, Summy JM, Lesslie DP, et al. Inhibition of SRC expression and activity inhibits tumor progression and metastasis of human pancreatic adenocarcinoma cells in an orthotopic nude mouse model. Am J Pathol 2006;168:962–72.
13. Windham TC, Parikh NU, Siwak DR, et al. Src activation regulates anoikis in human colon tumor cell lines. Oncogene 2002;21:7797–807.
14. Johnson FM, Saigal B, Talpaz M, Donato NJ. Dasatinib (BMS-354825) tyrosine kinase inhibitor suppresses invasion and induces cell cycle arrest and apoptosis of head and neck squamous cell carcinoma and non-small cell lung cancer cells. Clin Cancer Res 2005;11:6924–32.
15. Slack JK, Adams RB, Rovin JD, Bissonette EA, Stoker CE, Parsons JT. Alterations in the focal adhesion kinase/Src signal transduction pathway correlate with increased migratory capacity of prostate carcinoma cells. Oncogene 2001;20:1152–63.
16. Boyer B, Bourgeois Y, Poupon MF. Src kinase contributes to the metastatic spread of carcinoma cells. Oncogene 2002;21:2347–56.
17. Ellis LM, Staley CA, Liu W, et al. Down-regulation of vascular endothelial growth factor in a human colon carcinoma cell line transfected with an antisense expression vector specific for c-src. J Biol Chem 1998;273:1052–7.
18. Sato M, Tanaka T, Maeno T, et al. Inducible expression of endothelial PAS domain protein-1 by hypoxia in human lung adenocarcinoma A549 cells. Role of Src family kinases-dependent pathway. Am J Respir Cell Mol Biol 2002;26:127–34.
19. Playford MP, Schaller MD. The interplay between Src and integrins in normal and tumor biology. Oncogene 2004;23:7928–46.
20. Wong BR, Besser D, Kim N, et al. TRANCE, a TNF family member, activates Akt/PKB through a signaling complex involving TRAF6 and c-Src. Mol Cell 1999;4:1041–9.
21. Arron JR, Vologodskaia M, Wong BR, et al. A positive regulatory role for Cbl family proteins in tumor necrosis factor-related activation-induced cytokine (trance) and CD40L-mediated Akt activation. J Biol Chem 2001;276:30011–7.
22. Yu H, Jove R. The STATs of cancer-new molecular targets come of age. Nat Rev Cancer 2004;4:97–105.
23. Yu CL, Meyer DJ, Campbell GS, et al. Enhanced DNA-binding activity of a Stat3-related protein in cells transformed by the Src oncoprotein. Science 1995;269:81–3.
24. Kijima T, Niwa H, Steinman RA, et al. STAT3 activation abrogates growth factor dependence and contributes to head and neck squamous cell carcinoma tumor growth *in vivo*. Cell Growth Differ 2002;13:355–62.
25. Song JI, Grandis JR. STAT signaling in head and neck cancer. Oncogene 2000;19:2489–95.
26. Amann J, Kalyankrishna S, Massion PP, et al. Aberrant epidermal growth factor receptor signaling and enhanced sensitivity to EGFR inhibitors in lung cancer. Cancer Res 2005;65:226–35.
27. Gray MJ, Zhang J, Ellis LM, et al. HIF-1α, STAT3, CBP/p300 and Ref-1/APE are components of a transcriptional complex that regulates Src-dependent hypoxia-induced expression of VEGF in pancreatic and prostate carcinomas. Oncogene 2005;24:3110–20.
28. Johnson FM, Saigal B, Tran H, Donato NJ. Abrogation of signal transducer and activator of transcription 3 reactivation after Src kinase inhibition results in synergistic antitumor effects. Clin Cancer Res 2007;13:4233–44.
29. Saigal B, Glisson BS, Johnson FM. Dose-dependent and sequence-dependent cytotoxicity of erlotinib and docetaxel in head and neck squamous cell carcinoma. Anticancer Drugs 2008;19:465–75.
30. Sen B, Saigal B, Parikh N, Gallick G, Johnson FM. Sustained Src inhibition results in signal transducer and activator of transcription 3 (STAT3) activation and cancer cell survival via altered Janus-activated kinase-STAT3 binding. Cancer Res 2009;69:1958–65.
31. Cheng KW, Lu Y, Mills GB. Assay of Rab25 function in ovarian and breast cancers. Methods Enzymol 2005;403:202–15.
32. Hu J, He X, Baggerly KA, Coombes KR, Hennessy BT, Mills GB. Non-parametric quantification of protein lysate arrays. Bioinformatics 2007;23:1986–94.
33. Shah NP. Loss of response to imatinib: mechanisms and management. Hematology Am Soc Hematol Educ Program 2005;:183–7.
34. Deininger M, Buchdunger E, Druker BJ. The development of imatinib as a therapeutic agent for chronic myeloid leukemia. Blood 2005;105:2640–53.

Published OnlineFirst October 27, 2009; DOI: 10.1158/1078-0432.CCR-09-0767

35. Brown ER, Shepherd FA. Erlotinib in the treatment of non-small cell lung cancer. Expert Rev Anticancer Ther 2005;5:767–75.

36. Pao W, Wang TY, Riely GJ, et al. KRAS mutations and primary resistance of lung adenocarcinomas to gefitinib or erlotinib. PLoS Med 2005; 2:e17.

37. Engelman JA, Zejnullahu K, Mitsudomi T, et al. MET amplification leads to gefitinib resistance in lung cancer by activating ERBB3 signaling. Science 2007;316:1039–43.

38. Tsao AS, He D, Saigal B, et al. Inhibition of c-Src expression and activation in malignant pleural mesothelioma tissues leads to apoptosis, cell cycle arrest, and decreased migration and invasion. Mol Cancer Ther 2007;6:1962–72.

39. O'Sullivan LA, Liongue C, Lewis RS, Stephenson SE, Ward AC. Cytokine receptor signaling through the Jak-Stat-Socs pathway in disease. Mol Immunol 2007;44:2497–506.

40. Limnander A, Rothman PB. Abl oncogene bypasses normal regulation of Jak/STAT activation. Cell Cycle 2004;3:1486–8.

41. Lombardo LJ, Lee FY, Chen P, et al. Discovery of N-(2-Chloro-6-methyl-phenyl)-2-(6-(4-(2-hydroxyethyl)-piperazin-1-yl)-2-methylpyrimidin-4-ylamino)thiazole-5-carboxamide (BMS-354825), a dual Src/Abl kinase inhibitor with potent antitumor activity in preclinical assays. J Med Chem 2004;47:6658–61.

42. Morgan J, Demetri G, Wang D, et al. A phase I study of dasatinib, a Src multi-kinase inhibitor, in patients (pts) with GIST and other solid tumors. Eur J Cancer 2006;Suppl 4:118.

43. Johnson FM, Chiappori A, Burris H, et al. A phase I study (CA180021-Segment 2) of dasatinib in patients (pts) with advanced solid tumors. J Clin Oncol 2007;25:18S:14042.

44. Bantscheff M, Eberhard D, Abraham Y, et al. Quantitative chemical proteomics reveals mechanisms of action of clinical ABL kinase inhibitors. Nat Biotechnol 2007;25:1035–44.

45. Rix U, Hantschel O, Durnberger G, et al. Chemical proteomic profiles of the BCR-ABL inhibitors imatinib, nilotinib, and dasatinib reveal novel kinase and nonkinase targets. Blood 2007;110: 4055–63.

46. Purnell PR, Mack PC, Tepper CG, et al. The Src inhibitor AZD0530 blocks invasion and may act as a radiosensitizer in lung cancer cells. J Thorac Oncol 2009;4:448–54.

47. Pardanani A. JAK2 inhibitor therapy in myeloproliferative disorders: rationale, preclinical studies and ongoing clinical trials. Leukemia 2008;22:23–30.

48. Wernig G, Kharas MG, Okabe R, et al. Efficacy of TG101348, a selective JAK2 inhibitor, in treatment of a murine model of JAK2V617F-induced polycythemia vera. Cancer Cell 2008; 13:311–20.

49. Hexner EO, Serdikoff C, Jan M, et al. Lestaurtinib (CEP701) is a JAK2 inhibitor that suppresses JAK2/STAT5 signaling and the proliferation of primary erythroid cells from patients with myeloproliferative disorders. Blood 2008;111: 5663–71.

50. Kasper S, Breitenbuecher F, Hoehn Y, et al. The kinase inhibitor LS104 induces apoptosis, enhances cytotoxic effects of chemotherapeutic drugs and is targeting the receptor tyrosine kinase FLT3 in acute myeloid leukemia. Leuk Res 2008;32:1698–708.

AACR American Association for Cancer Research

Clinical Cancer Research

Reciprocal Regulation of c-Src and STAT3 in Non-Small Cell Lung Cancer

Lauren Averett Byers, Banibrata Sen, Babita Saigal, et al.

Clin Cancer Res Published OnlineFirst October 27, 2009.